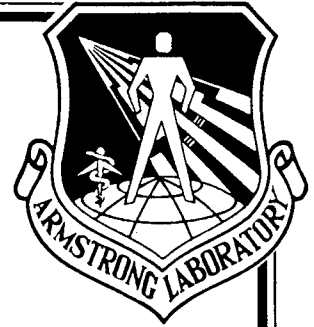
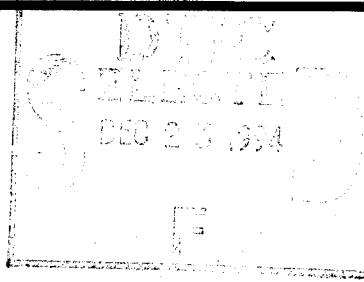


AL/CF-TR-1994-0116



**VISUAL CONTRAST DETECTION THRESHOLDS
FOR AIRCRAFT CONTRAILS (U)**

**Jeffrey A. Doyal
David P. Ramer**

**SCIENCE APPLICATIONS INTERNATIONAL CORPORATION
1321 RESEARCH PARK DRIVE
DAYTON, OH 45432**

**Michael D. Stratton
Bradley D. Purvis**

**CREW SYSTEMS DIRECTORATE
HUMAN ENGINEERING DIVISION
WRIGHT-PATTERSON AFB, OHIO 45433-7022**

JULY 1994

INTERIM REPORT FOR THE PERIOD DECEMBER 1993 TO JULY 1994

Approved for public release; distribution is unlimited

**AIR FORCE MATERIEL COMMAND
WRIGHT-PATTERSON AIR FORCE BASE, OHIO 45433-7022**

THIS REPORT IS UNCLASSIFIED

ARMSTRONG
LABORATORY
19941215 168

NOTICES

When US Government drawings, specifications, or other data are used for any purpose other than a definitely related Government procurement operation, the Government thereby incurs no responsibility nor any obligation whatsoever, and the fact that the Government may have formulated, furnished, or in any way supplied the said drawings, specifications, or other data, is not to be regarded by implication or otherwise, as in any manner licensing the holder or any other person or corporation, or conveying any rights or permission to manufacture, use, or sell any patented invention that may in any way be related thereto.

Please do not request copies of this report from the Armstrong Laboratory. Additional copies may be purchased from:

National Technical Information Service
5285 Royal Road
Springfield, Virginia 22161

Federal Government agencies and their contractors registered with the Defense Technical Information Center should direct requests for copies of this report to:

Defense Technical Information Center
Cameron Station
Alexandria, Virginia 22314

TECHNICAL REVIEW AND APPROVAL

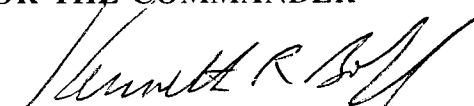
AL/CF-TR-1994-0116

This report has been reviewed by the Office of Public Affairs (PA) and is releasable to the National Technical Information Service (NTIS). At NTIS, it will be available to the general public, including foreign nations.

The voluntary informed consent of the subjects used in this research was obtained as required by Air Force Regulation 169-3.

This technical report has been reviewed and is approved for publication.

FOR THE COMMANDER



KENNETH R. BOFF, Chief
Human Engineering Division
Armstrong Laboratory

REPORT DOCUMENTATION PAGE			Form Approved OMB No. 0704-0188	
Public reporting burden for this collection of information is estimated to average 1 hour per response, including the time for reviewing instructions, searching existing data sources, gathering and maintaining the data needed, and completing and reviewing the collection of information. Send comments regarding this burden estimate or any other aspect of this collection of information, including suggestions for reducing this burden, to Washington Headquarters Services, Directorate for Information Operations and Reports, 1215 Jefferson Davis Highway, Suite 1204, Arlington, VA 22202-4302, and to the Office of Management and Budget, Paperwork Reduction Project (0704-0188), Washington, DC 20503.				
1. AGENCY USE ONLY (Leave blank)		2. REPORT DATE July 1994		3. REPORT TYPE AND DATES COVERED Interim Report Dec 93 - Jul 94
4. TITLE AND SUBTITLE Visual Contrast Detection Thresholds for Aircraft Contrails			5. FUNDING NUMBERS C: F33615-92-D-2293 PE - 62202F PR - 7184 TA - 10 WU - 45	
6. AUTHOR(S) Jeffrey A. Doyal David P. Ramer Michael D. Stratton Bradley D. Purvis				
7. PERFORMING ORGANIZATION NAME(S) AND ADDRESS(ES) Science Applications International Corporation (SAIC) 1321 Research Park Drive Dayton, OH 45432			8. PERFORMING ORGANIZATION REPORT NUMBER	
9. SPONSORING/MONITORING AGENCY NAME(S) AND ADDRESS(ES) Armstrong Laboratory, Crew Systems Directorate Human Engineering Division Human Systems Center Air Force Material Command Wright-Patterson AFB OH 45433-7022			10. SPONSORING/MONITORING AGENCY REPORT NUMBER AL/CF-TR-1994-0116	
11. SUPPLEMENTARY NOTES				
12a. DISTRIBUTION/AVAILABILITY STATEMENT Approved for public release; distribution is unlimited			12b. DISTRIBUTION CODE	
13. ABSTRACT (Maximum 200 words) Twenty licensed pilots participated in a laboratory investigation of visual detection thresholds for simulated aircraft contrails. Subjects searched a projection screen for simulated contrails while maintaining a prescribed flight profile on a simple flight simulator. Simulated contrails varied in width from 5 arc min of visual angle to 25 arc min, and varied in length from 2° to 10°. Subjects performed the detection task in an uncued condition, in which they searched an area measuring 135° x 37°; and in a cued condition, in which they searched an area measuring 45° x 37°. Detection thresholds decreased with increasing widths and length, however, thresholds were found to be higher than those demonstrated in previous studies. This difference is attributed to the use of a large visual search area and a secondary task. Cued detection, as described above, led to slightly lower detection thresholds. Psychometric functions were drawn that allow the reader to extrapolate the probability of detection associated with contrails of a given size and contrast.				
14. SUBJECT TERMS visual detection, contrast sensitivity, visual acuity, search contrails			15. NUMBER OF PAGES 53	
			16. PRICE CODE	
17. SECURITY CLASSIFICATION OF REPORT UNCLASSIFIED	18. SECURITY CLASSIFICATION OF THIS PAGE UNCLASSIFIED	19. SECURITY CLASSIFICATION OF ABSTRACT UNCLASSIFIED	20. LIMITATION OF ABSTRACT UNLIMITED	

THIS PAGE INTENTIONALLY LEFT BLANK

EXECUTIVE SUMMARY

Purpose

With the advances being made in stealth technology, radar and thermal signatures of aircraft are being greatly reduced. Thus, the visual signature of an aircraft, including the contrail it produces, can often be the most conspicuous signature emitted. In order to maximize system survivability, it is essential to understand the nature of visual detection of contrails and to predict when contrails are most likely to be detected. This study was conducted in order to begin to quantify aspects of visual contrail detection in an air-to-air scenario. Specifically, its purpose was to assess how contrail detection varies as a function of contrail length, contrail width and observer cueing.

Method

Twenty licensed pilots performed a contrail detection task in a laboratory setting. Subjects searched a $135^{\circ} \times 37^{\circ}$ projection screen for simulated contrails, while at the same time performing a simulated flight task. This approach was selected in an effort to present a realistic air-to-air search scenario. Using an increasing method of limits, measures of luminance contrast at detection were collected for simulated contrails that varied in width and length from a smallest contrail condition of 5 arc min. \times 2° , to a largest condition of 25 arc min. \times 10° . In addition, thresholds were collected for contrails that could appear anywhere within a $135^{\circ} \times 37^{\circ}$ area (uncued detection) or for contrails that appeared in only a $45^{\circ} \times 37^{\circ}$ area (cued detection).

Results and Discussion

Detection thresholds were found to decrease as a function of increasing contrail size, with significantly lower thresholds being exhibited for each increase in length and width. The effect of increasing stimulus size on percent contrast at detection decreased and began to reach an asymptote for the largest contrail sizes tested. See Figure ES-1. Cued detection also led to slightly lower detection thresholds than did uncued contrail detection. However, thresholds in

both cueing conditions were found to be much higher than in previous visual detection studies. Researchers attribute this difference to the fact that the current scenario included both a visual search component and a secondary task in addition to the stimulus detection task. These components, though not introduced in previous studies, were essential to creating a realistic air-to-air search scenario. This data can be presented in the form of psychometric functions that can help the reader to predict the probability of detection associated with a contrail of a given size and contrast.

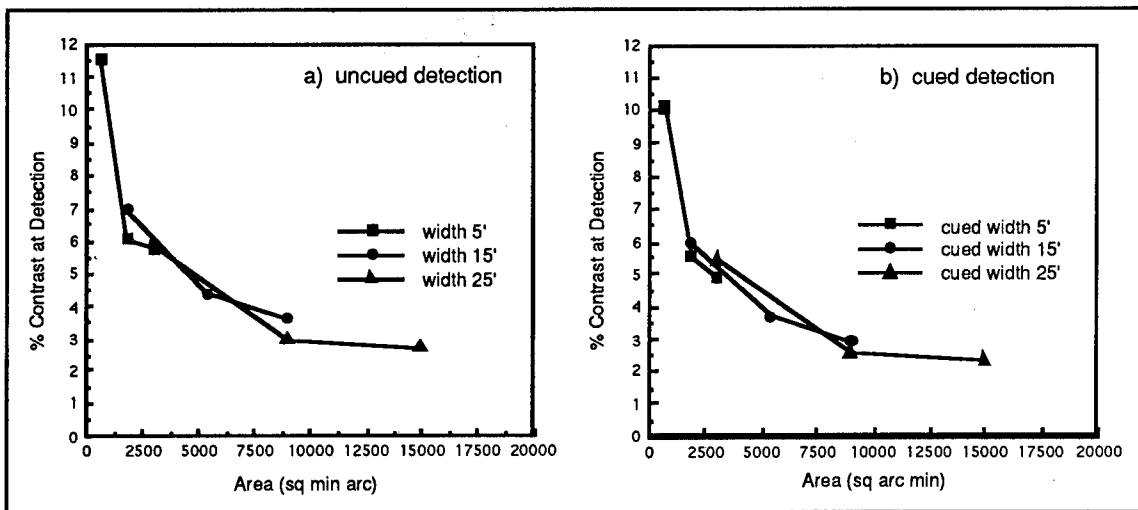


Figure ES-1. Detection Threshold as a Function of Contrail Area for Uncued (a) and Cued (b) detection.

PREFACE

The research effort described in this report was performed by Science Applications International Corporation (SAIC) under the Systems Engineering Design and Technical Analysis Contract Number F33615-92-D-2293, Systems Integration Design and Evaluation Facility (SIDEF). The work was performed at the Armstrong Laboratory, Crew Systems Directorate, Human Engineering Division, Crew Systems Integration Branch (AL/CFHI), Wright-Patterson AFB, OH.

Acknowledgment is made to the following personnel who contributed many ideas and hours to the successful completion of this effort.

From Armstrong Laboratory (AL/CFHI);
Mr. Earl Sharp

From the B-2 System Program Office (SPO) at Wright Patterson AFB;
Capt Ron Schrupp

From Northrop Corporation, Pico Rivera, CA;
Mr. Bob Rubin
Dr. Pat Saatzer

From Science Applications International Corporation (SAIC) in Dayton, OH;
Mr. Greg Bothe Sr.
Mr. Tom Haberlandt
Dr. Gregg Irvin
Mr. Roger Overdorf
Mr. Mike Sargent
Mr. John Stengel

Accession For	
NTIS CRA&I	<input checked="checked" type="checkbox"/>
DTIC TAB	<input type="checkbox"/>
Unannounced	<input type="checkbox"/>
Justification	
By	
Distribution	
Availability	
Doc	Notes
A-1	

TABLE OF CONTENTS

LIST OF FIGURES	vii
LIST OF TABLES	viii
LIST OF SYMBOLS, ABBREVIATIONS, AND ACRONYMS	ix
SECTION I.....	1
Purpose	1
Background	1
Approach	6
Assumptions	7
SECTION II.	8
Subjects	8
Apparatus.....	8
Experimental Design	10
Stimuli	10
Contrast.	11
Simulated Sky Characteristics.	11
Simulated Contrail Characteristics.....	15
Procedure.....	17
Simulated flight task.	17
Contrail detection task.	18
Data Collection Procedure.	21
SECTION III.....	23
Descriptive and Inferential Statistics	23
Psychometric Functions	26
SECTION IV.	30
Threshold Values	30
Effect of Stimulus Area.....	30
Generalizability	33
SECTION V.	35

LIST OF FIGURES

Figure 2.1.	Experimental Configuration	9
Figure 2.2.	Luminance Profile of LCD Projectors Measured at Screen Before (a) and After (b) Correction.	12
Figure 2.3.	Spectral Luminance of the Sky	13
Figure 2.4.	Illustration of Contrail and Sky Color Plotted in CIE 1931 Color Space.....	14
Figure 3.1.	Main Effect of Cueing.....	24
Figure 3.2.	Main Effects of Width (a and b) and Length (c and d)	25
Figure 3.3.	Interactions Between Contrail Width and Length for Uncued (a) and Cued (b) Detection.....	25
Figure 3.4	Psychometric Data and Quick Curves for Uncued Condition	27
Figure 3.5	Psychometric Data and Quick Curves for Cued Condition	28
Figure 4.1.	Detection Threshold as a Function of Contrail Area for Uncued (a) and Cued (b) Detection.....	31
Figure 5.1.	Mean Thresholds at Detection for the Experimental Conditions and Extrapolated to 1 Arc Min Using a Best Fit to Piper's Equation	37
Figure 5.2.	Predicted 10% Probability of Detection Curves	38
Figure 5.3.	Predicted 50% Probability of Detection Curves	39
Figure 5.4.	Predicted 100% Probability of Detection Curves	40

LIST OF TABLES

Table 2.1. Contrast Values Presented for Each Experimental Condition	20
Table 3.1. Mean Luminance Contrast at Detection	23
Table 3.2. S and β Values for Each Experimental Condition.	29
Table 5.1. K Constants for Detection Criteria.	36

LIST OF SYMBOLS, ABBREVIATIONS, AND ACRONYMS

ADMPS	Advanced Defensive Mission Planning System
AL/CFHI	Armstrong Laboratory, Crew Systems Directorate, Human Engineering Division, Crew Systems Integration Branch
APU	Auxiliary Processing Unit
CAP	Combat Air Patrol
CPU	Central Processing Unit
ETACFCST	United States Air Forces in Europe, Tactical Air Command Algorithm for Forecasting Contrails
LCD	Liquid Crystal Display
MFD	Multi-function Display
MIP	Mission Initial Point
PC	Personal Computer
P&ES	Prototyping and Evaluation System
SAIC	Science Applications International Corporation
SG	Silicon Graphics
SPO	Systems Program Office
VAPS	Virtual Avionics Prototyping System
VSD	Vertical Situation Display

THIS PAGE INTENTIONALLY LEFT BLANK

SECTION I. INTRODUCTION

Purpose

For years, a great deal of time and resources have been allocated to developing radar and infrared (IR) systems that can detect enemy aircraft at long ranges in an air-to-air scenario. These systems generally allow detection at greater distances than is possible using only the naked eye. With the recent advances in stealth technology, however, radar and thermal signatures of aircraft are being greatly reduced, and consequently, the effectiveness of these sensor systems is becoming more limited. This has resulted in the fact that the visual signature of an aircraft can sometimes be the most likely to be detected, which places emphasis once again on visual detection by the human observer. Condensation trails, or *contrails*, are perhaps the most conspicuous visual cue emitted by an aircraft, often being visible at a far greater distance than the aircraft itself. As one might suspect, in air-to-air engagements such contrail formation will increase the probability of detection of aircraft by allowing a pilot to vector in to the area in which the aircraft is located. For this reason, it is clearly desirable to understand and characterize human visual detection of aircraft contrails, and to apply this knowledge to the design of systems and procedures intended to reduce possibility of visual contrail detection.

The purpose of the current study was to obtain performance data in an attempt to quantify various aspects of human visual detection of aircraft contrails. Specifically, researchers sought to understand how detection thresholds are affected by such factors as contrail width, contrail length and observer cueing in an air-to-air operational setting.

Background

Contrails can be defined as elongated, tubular clouds composed of super-saturated air that forms in the wake of an aircraft (Air Weather Service, 1981). The two predominant forms of contrails are "aerodynamic" contrails, which form due to a rapid decrease in pressure caused by air traveling over an airfoil, and

"engine-exhaust" contrails, which form when the water vapor in the exhaust gas mixes with and saturates the air in the wake of the aircraft (Appleman, 1953). It is the latter type of contrail that can be seen stretching for miles across the sky and that is most vulnerable to visual detection.

The majority of previous contrail research has focused upon predicting the environmental conditions under which contrails will be formed, including relative humidity, initial pressure, and temperature. Herbert Appleman developed predictive curves depicting critical temperature for contrail formation as a function of pressure, relative humidity, and the amount of air entrained into aircraft exhaust, regardless of aircraft type, fuel, or power settings (Bjornsen, 1992). Later, Bjornsen developed a new contrail forecasting technique called ETACFCST (United States Air Forces in Europe, Tactical Air Command Algorithm for Forecasting Contrails) which utilizes discriminant analysis schemes to obtain a "best-fit" prediction curve of contrail formation as a function of altitude and temperature, or temperature and vertical motion. These predictions were later modified to include an aircraft engine "fuel to air" ratio.

This valuable research has resulted in the capability to determine whether or not an aircraft contrail will be produced under a given set of atmospheric conditions. However, it provides only one half of the solution to understanding the extent to which aircraft are vulnerable to visual detection. In addition to knowing when, a visual stimulus will be produced, it is necessary to understand the parameters that affect human visual detection of that stimulus.

Perhaps one of the most salient factors that impact contrast detection thresholds for any object is stimulus size. Two of the classic and most significant studies investigating this issue were conducted by Ricco (1877) and Piper (1903). In an attempt to characterize the relationship between stimulus size and contrast detection thresholds, Ricco developed an equation that accurately predicts thresholds for a range of small-area targets. This equation, known as Ricco's law is shown below in Equation 1.1, where: I is the intensity per unit retinal area required for detection, A is the stimulus area and k is a constant.

$$I = \frac{k}{A} \quad \text{Eq. 1.1}$$

This law of spatial integration has been shown to hold for targets up to 10 arc min in diameter for foveal viewing and 200 arc min in the periphery (Graham, Brown & Mote, 1939, cited in Brown & Deffenbacher, 1979). Piper (1903) expanded upon this finding, developing an equation (Piper's Law) that characterizes the relationship between target size and contrast detection thresholds for slightly larger stimuli. Piper's law, which has been shown to accurately describe contrast detection thresholds for stimuli ranging between 10 and 60 arc min in diameter in the fovea and 3.3° to 10° in the periphery, is shown below in Equation 1.2 (Graham et al., 1939, cited in Brown & Deffenbacher, 1979). This formula shows a diminishing effect of increasing stimulus area in that contrast detection thresholds decrease with the *square* of the area.

$$I = \frac{K}{A^2} \quad \text{Eq. 1.2}$$

Eventually, as stimulus size increases beyond the bounds of Ricco's area and Piper's area, the relationship between stimulus area and contrast detection thresholds disappears. That is, for objects over a given size, increasing stimulus size does not impact the degree of luminance contrast required to detect the stimulus.

A considerable amount of basic visual research has also investigated target detection thresholds for various spatial patterns. Much of this research resulted from military interest during W.W.II. Perhaps most directly relevant to the current investigation, Lamar, Hecht, Schlaer and Hendley (1947) conducted a comprehensive study of detection thresholds for rectangular stimuli that varied in length/width ratio as well as stimulus area. In this study, Lamar et. al. found that the ratio of length to width is not an important determinant of detection thresholds for stimuli that have small to moderate asymmetries (i.e. low-moderate length/width ratios). For such stimuli, *area* was found to be the critical factor driving stimulus detection. When viewing stimuli with high length/width ratios, however, contrast thresholds were affected more by stimulus asymmetry. Thresholds were found to increase with length/width ratio for longer, narrower targets. Interestingly, Lamar et. al. also found that increasing the target area, which decreased thresholds significantly for smaller targets, had diminishing

impact on detection thresholds for larger targets (exceeding 100 sq arc min. of visual angle).

Another classic study investigating visual detection of low-contrast targets was performed by Blackwell (1946). This study, which used circular stimuli between 3.5 and 120 arc minutes in diameter, investigated target detection thresholds as a function of target area and luminance adaptation level. Results from this investigation showed that for the largest field sizes, the effect of adaptation level on contrast at detection is constant across adaptation levels of 1.0 to 100 footlamberts. In addition to studying thresholds for stimuli that are brighter than the background (positive contrast), Blackwell also used stimuli that had lower luminance levels than the background (negative contrast). In general, thresholds for detection of negative contrast stimuli were equivalent to those for positive contrast stimuli, with the exception that large stimuli at low adaptation levels elicited thresholds 20 percent lower than those for positive contrast targets.

A related aspect of target detection that was actively investigated during the W.W.II era is the visibility of distant objects. Researchers became interested in predicting the detection thresholds for objects viewed through the atmosphere. Over a distance, the atmosphere can attenuate target/background contrast by scattering and absorbing not only the light emitted from the object, but also that of the ambient daylight. Duntley (1948) proposed a set of rules that govern detection of objects viewed along an upward, downward or horizontal line of sight. This work has allowed subsequent researchers to estimate the reduction in apparent contrast of an object and the associated increase in inherent contrast required for detection.

Finally, a good deal of research has also addressed the issue of spatial uncertainty and how it impacts detection thresholds. A commonly held theory on spatial uncertainty and how it relates to the detection is that of visual lobes (Overington, 1976). This theory, resulting from a large body of research, states that the visual system can only detect a given object within an area around the foveal region known as the visual lobe. The visual lobe is defined as the area around the fovea in which detection of a given object is 50% of that of the fovea. For a subject searching a large viewing area such as the open sky, the visual lobe is moved around this search area until the object is located. The search

time is related to the size of the search area and inversely related to the size of the visual lobe. The size of the visual lobe is different for objects having different characteristics including size and contrast. Thus, as target size and/or contrast decreases, the size of the visual lobe decreases, thereby increasing visual search time for the target. If search time is limited, resulting in a reduced amount of sampling from the visual lobe, probability of detection will also become limited.

Each of these areas of research plays an important role in characterizing visual contrail detection. However, due to the extreme complexity of contrail formation, atmospheric attenuation, and human visual detection, previous research has only begun to solve the puzzle of predicting contrail detection. For example, it can be extremely difficult to characterize the contrail itself. Contrails vary widely in their size depending upon the size of the aircraft engine, atmospheric conditions, and viewing distance. They can be straight or curved, solid or intermittent, and can have positive or negative contrast. They are typically wider at one end than the other and may be made up of one, two or even four distinct contrails emanating from the engines that merge into a single larger contrail further behind the aircraft. Further, a single contrail undergoes changes over time. From the time they are first generated, they spread out in area while their contrast against the sky decreases. Contrast also varies as a function of viewing distance. As the distance between the observer and the contrail increases, there is more opportunity for atmospheric attenuation, which serves to scatter the light reflecting from the contrail as well as the ambient light, thereby reducing the apparent contrast of the contrail. The specific dynamics of these factors and the resulting conspicuousness of the contrail are impacted by a number of atmospheric characteristics including air temperature, humidity, visibility and cloud cover (Air Weather Service, 1981.)

In addition to the many variables inherent to the physical characteristics of contrails, the characterization of contrail detection is also made difficult by a number of factors inherent to human visual perception. Not only is visual detection impacted by factors of target size and spatial uncertainty described above, but it is also determined by factors such as target orientation, velocity, light adaptation and location in the visual field, which interact to determine the probability of target detection (Boff & Lincoln, 1988). This broad range of

variables presents a formidable challenge to researchers pursuing the accurate and comprehensive characterization of visual contrail detection.

Approach

Obviously, the task of characterizing the effects of all of these variables on contrail detection within the scope of a single study would not be feasible. Thus, the current study focused on manipulating only a subset of these variables including contrail width and length (target size) and observer cueing (spatial uncertainty). As it is well understood that these factors affect target detection thresholds, the purpose of this study was not to test hypotheses, but rather to quantify the effects of contrail width and length and observer cueing within a specific scenario. That is, the effects of size and spatial uncertainty were examined while such variables as orientation, target velocity, light adaptation, and location in the visual field were either held constant or randomized, and their effects were not examined.

The experimental approach consisted of a three-factor experiment investigating the effect of contrail width and length on contrail detection as well as the effect of observer cueing. Detection thresholds for simulated contrails, in terms of the percent luminance contrast between the contrail and sky, were examined as a function of these three variables. In an effort to more accurately represent a typical air-to-air visual search task, subjects were required to perform the detection task and a simple flight task simultaneously. These two tasks are described in detail in Section II.

Assumptions

Due to the complex nature of contrail characterization and the numerous factors that influence visual target detection, a number of up-front assumptions were made that helped to narrow the scope of the investigation and to concentrate on areas considered to be of primary importance. These assumptions, listed below, were developed jointly among researching parties during the early stages of the contrail study planning.

- The investigation was to address the luminance contrast required for visual detection of a contrail.
- The investigation was to address the effects of only three variables: contrail width, contrail length, and observer cueing.
- Color and luminance were to be uniform across the background and across the contrail (i.e. solid contrail against a cloudless, uniform sky.)
- Sky and contrails were to be simulated using projection of computer-generated imagery.
- Subjects were to be light adapted at room-lighting level, not at bright daylight level.
- Subjects were to perform a nominal level of flight task simultaneously with the visual search task.
- Subjects would have no more than 8 seconds exposure to each contrast condition within a trial.

These assumptions helped to define the study as an investigation of human visual detection ability and eliminated the need to conduct more complex contrail modeling activities.

SECTION II. METHOD

Subjects

A total of twenty subjects, 18 male and 2 female, participated in the study. Approximately half of the subjects were civilian and military members of the Aero Club at Wright-Patterson Air Force Base (W.P.A.F.B.) in Dayton, OH, and were current licensed pilots. The remaining subjects were current USAF pilots stationed at W.P.A.F.B. As such, each subject had passed an annual physical and had been tested for 20/20 corrected visual acuity. In addition, prior to participation in the study, each subject was screened for normal contrast sensitivity using a Pelli-Robson contrast sensitivity chart. The minimum allowable performance on this test was selected as a Weber contrast threshold of .01122 (log contrast sensitivity of 1.95) with binocular viewing. (One subject failed to meet this criterion and did not participate in the data collection.)

Apparatus

The experimental stimuli consisted of simulated aircraft contrails presented against a sky-colored background. Both the contrails and the background were generated on a Silicon Graphics Iris 4D/320 VGX workstation, and the RGB imagery was subsequently run through a YEM CVS-980 scan converter to create a Super-VHS video signal. This video was then recorded frame by frame onto high-density optical disks using a Panasonic TQ-2022FC optical memory disk recorder. The optical disks were played back using three Panasonic LQ3032T optical disk players, and the imagery was projected through three Panasonic XG-H400U LCD projectors onto a 30 ft. x 100 in., matte white Da-Lite projection screen. The screen was hinged at a 45° angle at ten foot intervals such that it formed three adjacent sections measuring ten feet wide by 100 in. high. Imagery from each projector fell on a separate section of the screen. The three optical disk players were controlled by a 386 personal computer (PC), which served as the experimenter workstation. Subject responses were made on a three-button mouse and recorded on the PC. Due to the distance between the cockpit and experimenter station and high ambient noise levels, headsets with microphones were worn by the subject and experimenter to facilitate communication.

The flight simulation portion of the task was conducted using the B-2 Prototyping and Evaluation System (P&ES). This system consists of a simple cockpit with stick, rudder pedals, and throttle quadrant. The flight simulation model was hosted on a Concurrent 3260 MPS computer consisting of a CPU and four Auxiliary Processing Units (APU's). An Ethernet backbone (802.3) was used to connect the Concurrent to each of 3 Silicon Graphics Units (two model 4D-310 GTXs and a model 4D-320 VGX) and a linkage processor. The P&ES cockpit included only a vertical situation display (VSD). This display was developed using Virtual Prototype's Virtual Avionics Prototyping System (VAPS) hosted on a Silicon Graphics Iris 4D/310 GTX workstation, and was presented on a 6" X 6" multiple function display (MFD) screen mounted directly above the stick such that the subjects viewed the display in a head-down position. A diagram of the experimental configuration can be seen in Figure 2.1.

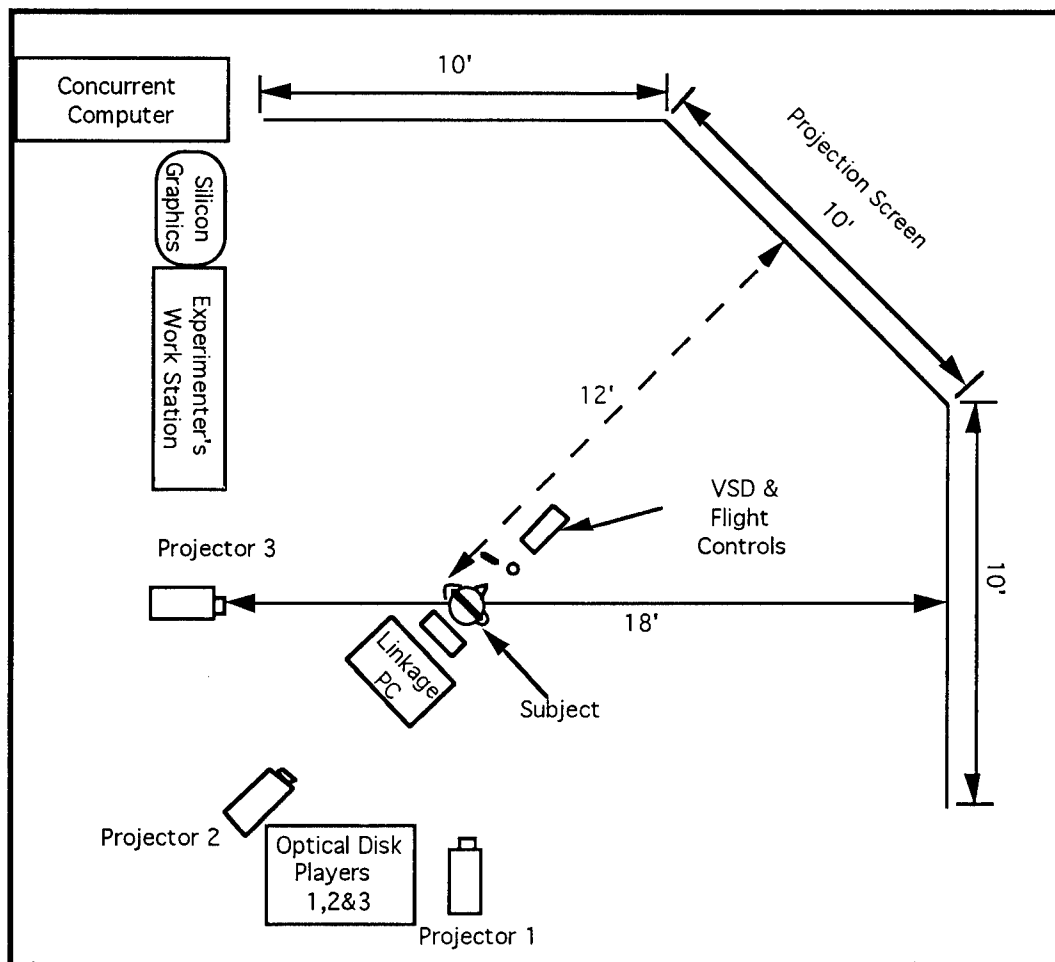


Figure 2.1. Experimental Configuration

Experimental Design

The experiment consisted of a contrail detection task that took place concurrently with a simulated flight task in an attempt to mimic a real-world scenario in which an interceptor aircraft pilot was searching for contrails of other aircraft. This study examined the contrast detection threshold for simulated contrails of three widths and three lengths. In addition, it examined these thresholds as a function of whether the observer was cued (knew approximately where in the visual field the contrail would appear) or uncued (did not know where the contrail would appear). This resulted in a 3 x 3 x 2 factor study. All contrails were presented in a horizontal orientation and were placed in random locations on a 135° projection screen.

The experiment used an ascending method of limits approach to determine thresholds and was implemented using a repeated measures design, exposing each of the subjects to all 18 combinations of the independent variables. Each experimental condition was observed six times, resulting in a total of 108 data collection trials per subject, and a total of 2160 trials in all.

Stimuli

Researchers attempted to establish a *conservative* estimate of visual detection thresholds for aircraft contrails. To accomplish this, an effort was made to develop a worst-case scenario in terms of contrail visibility. That is, a scenario was developed in which long, wide contrails were being emitted against a cloudless blue sky. Because clouds serve to distract and confuse the observer, as well as to decrease the contrast of the contrail, a clear blue sky was used as the background for this study. The following is a discussion of the various components of the experimental stimuli, including the procedures for determining and verifying luminance contrast and color of the simulated sky and contrails, as well as the selection of shape and size of the contrails.

Contrast. Although white contrails differ in color from a blue sky, the primary factor driving visual detection of contrails and most other objects is the luminance contrast between the target and background. There are two commonly accepted concepts of contrast: contrast ratio and Michelson, or modulation, contrast. Within each concept and its definition, there are variations on how the light and dark areas or target and background are treated. Michelson contrast is typically reserved for spatially modulating stimuli, such as sine waves. For a single target on a uniform background such as a contrail, *contrast ratio* is most commonly used. The definition for contrast that will be used throughout this paper is contrast ratio described in the equation below:

$$Contrast = \frac{(L_T - L_B)}{L_B} \quad \text{Eq. 2.1}$$

Where: L_T is the luminance of the target and L_B is the luminance of the background. Values greater than 0.0 indicate a target that is brighter than the background, and values less than 0.0 indicate a target that is less luminous than its background. These conditions are often referred to as *positive* and *negative* contrast respectively. The current study examined only conditions in which a contrail exhibited positive luminance contrast in relation to the sky.

Simulated Sky Characteristics. The luminance of the blue sky can be as bright as 10^4 cd/m² (RCA, 1974). This is not easily achievable in the laboratory situation as there is little commercial equipment which will achieve these high brightness levels. The XG-H400U projectors used to project the experimental stimuli were found to be among the brightest large-area display units available within the budget of this effort.

To maximize the luminance of the background, and to achieve photopic adaptation in the subject, room lighting was left on during the conduct of the study. Baffles were placed on the room lights to reduce shadowing that would create non-uniformities on the projection screens. The intensity of this lighting was controlled by a potentiometer and set to the highest level that would still allow a target/background contrast that was well above threshold using the

maximum luminance output of the projectors. Measured at the subject position, the ambient room lighting was 113 Lux.

Unfortunately, the luminance of the projectors was not uniform across their display area. To measure this non-uniformity, room lights were turned off and a uniform white stimulus (RGB = 255, 255, 255) was presented on each screen. The luminance of each screen was measured in 64 separate locations (seven vertical by eight horizontal positions). Each projector exhibited roughly the same luminance profile, which included a distinct hot spot in the center that was approximately three times brighter than at the far periphery of the screen. This luminance profile can be seen in Figure 2.2a. To correct for this non-uniformity, a Gaussian neutral density filter was constructed and attached to the lens of each projector. This resulted in a corrected luminance profile for the three projectors, illustrated in Figure 2.2b. (Note that the luminance measures were used for calibrating uniformity across the projected imagery and differ from the luminance measures of the actual experimental stimuli.)

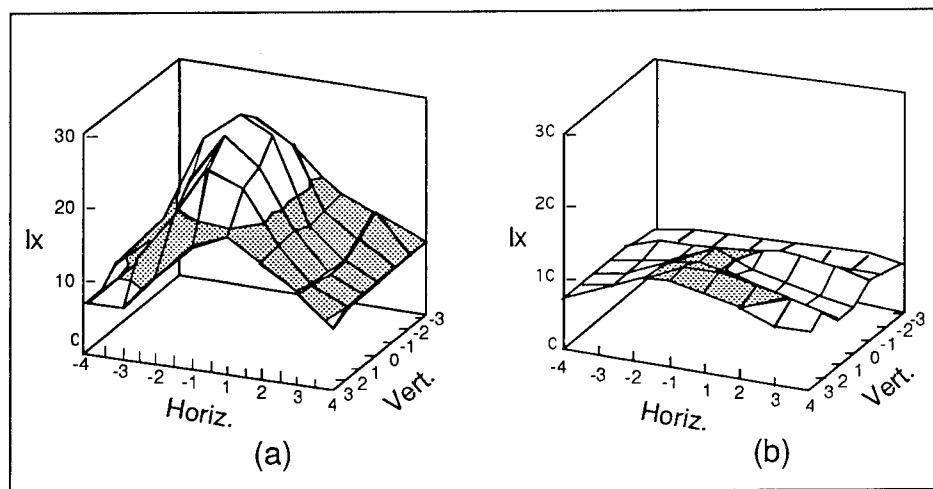


Figure 2.2. Luminance Profile of LCD Projectors Measured at Screen Before (a) and After (b) Correction.

Once a uniform luminance distribution from the projectors had been approximated, color and luminance values for the sky were selected.

The apparent color of the sky is a result of Rayleigh scattering. This scattering occurs with particles that are small compared to the wavelength of light, such as the gases in the atmosphere (Meyer-Arendt, 1972). Rayleigh scattering is a wavelength-dependent quantity, scattering blue light more strongly than red, thereby causing the bluish appearance of the sky. A spectral curve of blue sky is provided in Figure 2.3 (RCA, 1974). This curve was used to determine an approximate blue sky color to be used as a background in the experiment. A color coordinate was obtained by digitizing the curve and subsequently inputting its data into the 1931 Commission International de l'Eclairage (CIE) color model, which incorporates the tristimulus curves of the human eye. The color coordinate that resulted was $x=0.24$, $y=0.25$, which served as the background color and is illustrated in color space in Figure 2.4.

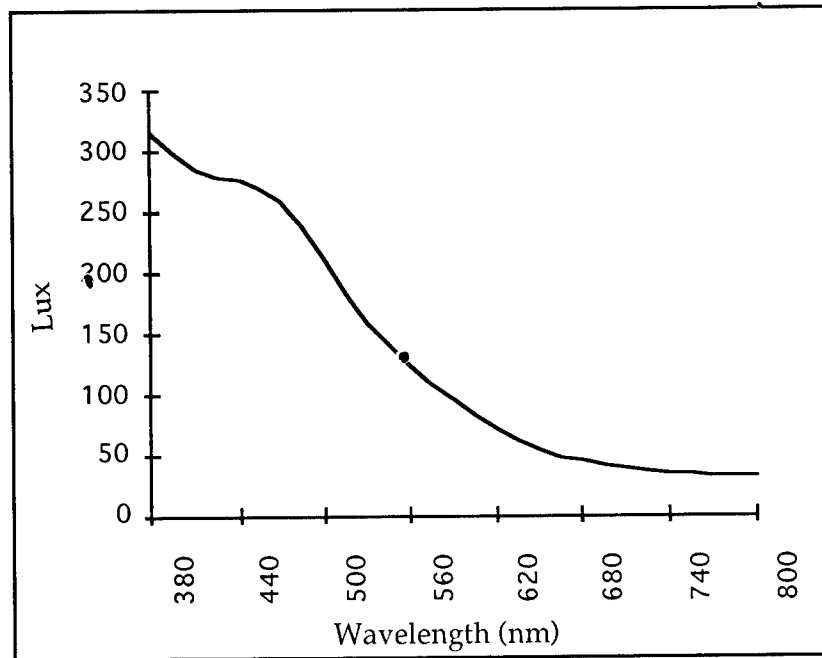


Figure 2.3. Spectral Luminance of the Sky

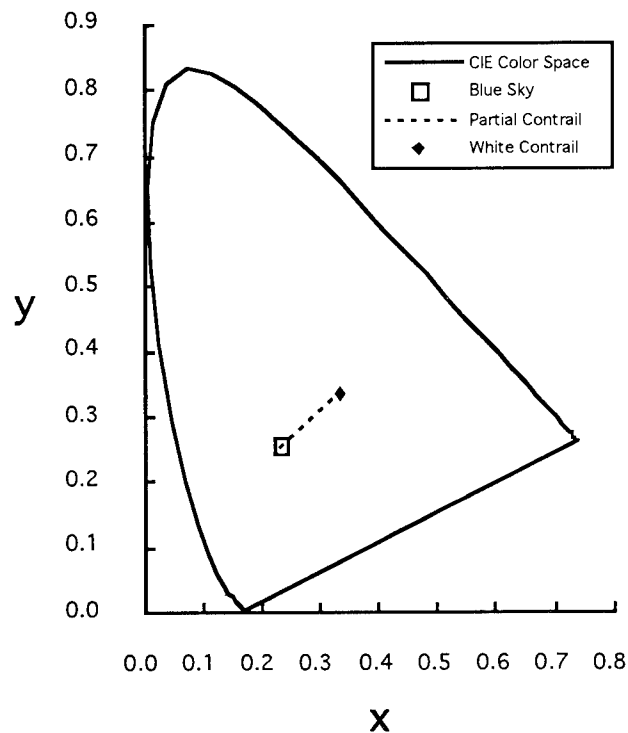


Figure 2.4. Illustration of Contrail and Sky Color Plotted in CIE 1931 Color Space

Imagery for both the sky and contrails was generated on the Silicon Graphics computer. The imagery was then projected onto the screen through the Sharp XG-H400U LCD video projectors. Because the colors displayed by the projectors are not necessarily the same as those on the SG monitor, and because room lights were kept on during experimentation causing ambient light to fall on the projection screens, calibration of the sky color was conducted empirically from the screens. The three projectors were adjusted such that they demonstrated equivalent color responses for a given input. To achieve maximum luminance of the projected background, the blue component of Silicon Graphics monitor RGB levels was set to 100%. The red and green RGB components were then adjusted until values on the projection screen, measured by a Minolta Chroma Meter, approximated $x=0.24$, $y=0.25$, the color value of the blue sky. The RGB inputs required to achieve this color were 80, 80 and 255, respectively. The projected background and ambient lighting resulted in a luminance adaptation level of 2.11 footlamberts, which was the maximum level achievable that would

still allow a sufficient adjustment range to produce a contrail/sky luminance contrast that was well above threshold.

Simulated Contrail Characteristics. Once parameters for the background had been determined, the simulated contrails were developed. Aircraft contrails, when first generated, appear bright white when viewed against a blue background such as the selected sky color described above. However, when contrails begin to dissipate over time, their apparent color tends to shift to that of their background. A contrail consists of tiny water droplets and ice particles which scatter the light from the sun using a mechanism called "Mie" scattering (Meyer-Arendt, 1972). This wavelength-independent form of scattering occurs when the particles are about the same size as the wavelength of light being scattered. All wavelengths are scattered equally making the contrail appear white. If a contrail contains a densely packed distribution of these water and ice particles, its contrast is high and it appears opaque. However, as the number and density of these scattering particles is reduced, the contrast is reduced, and the contrail begins to become transparent. As this dissipation occurs, the light from the blue sky and white light scattered off the particles in the contrail are superimposed.

Atmosphere between a contrail and the observer is another means by which a contrail's contrast is reduced. Although at the location of the contrail, visual contrast may be high, this contrast will be attenuated as the observer-to-contrail distance increases. This is due to the scattering of the atmosphere between the contrail and observer.

When two colors are superimposed they create a new color on a straight line in color space between the original colors. The point on that line where the new color appears is dependent upon the relative intensity of the original two colors. In this specific case, the sky intensity is constant, but the white light scattering from the contrail varies. A contrail that is unobservable does not scatter enough white light to significantly change the contrast or color from the sky blue background. As the contrail scatters more light, the contrast increases and the color of the contrail shifts along a line from blue to white.

To accurately display the contrail using the video system, the contrast must change as the color shifts along a line in color space between the blue sky and white. The following equations give the intensity of the RGB display components for a given contrail intensity:

$$R = (R_{\text{Max}} - R_T) \Delta I + R_S \quad \text{Eq. 2.2}$$

$$G = (G_{\text{Max}} - G_T) \Delta I + G_S \quad \text{Eq. 2.3}$$

$$B = (B_{\text{Max}} - B_T) \Delta I + B_S \quad \text{Eq. 2.4}$$

Where:

R_{Max} , G_{Max} and B_{Max} are the maximum RGB values

R_S , G_S and B_S are the RGB values for sky blue, and

ΔI is the change in intensity, which is related to contrast.

Rather than inserting contrast directly into the equations, ΔI is used because the contrast for specific RGB values does not deliver consistent results across all video displays. The practice of the above equations is shown in Figure 2.4, which illustrates the CIE 1931 color space with the path followed by the contrail color coordinate for varying contrast levels.

Although Gaussian filters on the projectors and baffles on the room lighting helped to improve the luminance uniformity, small non-uniformities still existed. This problem required the direct measurement of the contrast at each area of the screen. The contrast was measured empirically at multiple locations on each section of each projection screen using a Photo Research Pritchard 1980 photometer/colorimeter and relating contrast to ΔI . To accomplish this, each section was divided into nine target areas in which contrail contrast was measured. A photometer was positioned to measure a given contrail luminance at a specific computer contrast setting. The contrail was then removed, and the luminance of the sky (background) was measured without repositioning the photometer. This procedure was repeated at 27 independent locations across the entire screen. The photometer was equipped with a slit viewing area for measuring linear targets, which permitted the integration of more than ten video pixels in the condition of the thinnest contrail. From this data, a linear

relationship between empirically-measured contrast in a specific area of the screen and the computer contrast setting used to generate the contrails was identified. This linear relationship was subsequently confirmed with repeated contrast measurements. The entire calibration process was conducted under the experimental lighting conditions. In addition, there was no effect of contrail width or length on contrail contrast, enabling a single calibration to be used for contrails of all sizes displayed within a single given target area. Preliminary data collection confirmed this work by showing similar detection contrasts for different areas of the screen.

The width of the contrails capable of being produced was limited by the resolution of the projection systems. At projection distances of eighteen feet, the minimum distance that allowed the three systems to cover an area of 135° measured at the point of the observer, the minimum achievable contrail width was 5 arc min. This width was chosen to be the narrowest of three contrail width conditions. In order to span a range of possible contrail sizes, widths of 15 arc min. and 25 arc min. were selected as medium and high-width conditions respectively. The three levels of length chosen included 2° , 6° and 10° , which were also thought to be representative of a typical contrail viewing scenario. The size ratio (1:3:5) of these lengths to one another matched that among widths.

Procedure

The experimental procedure consisted of two concurrent tasks. The subject was required to fly a defined flight profile on a simulator while visually searching for contrails projected on a screen in front of him/her. These tasks are described below:

Simulated flight task. The purpose of the flight task was to create a realistic air-to-air visual search scenario in terms of head-up vs. head-down time. A pilot flying combat air patrol (CAP), for example, spends a great deal of time scanning the sky for signs of other aircraft, however, he also periodically scans his instrument panel and sensor screens. Therefore, a flight task was developed that would require the subjects to periodically interrupt their visual scan to glance down and monitor the cockpit.

The flight task activity involved maneuvering an airborne aircraft to a number of mission initial points (MIPS). A flight pattern, developed using the Advanced Defensive Mission Planning System (ADMPS), consisted of a simple figure eight pattern spanning 32 MIPS positioned approximately 15 naut. mi. apart. This mission was then transferred to the Concurrent computer system and integrated into the flight simulation. With no out-the-window cues, subjects received all guidance and feedback from a vertical situation display (VSD) presented on a MDU positioned in front of them. The VSD provided magnetic heading, speed, altitude, radar altitude, an artificial horizon, and a pitch ladder. In addition, at the top of the display was a commanded-heading flight director. This floating symbol indicated the commanded heading at which the subject must fly to reach each MIP and to follow the desired flight path. The subject's task was to make the required control inputs based on commanded headings from the flight director. Altitude and throttle inputs were held steady by the system, and therefore required no adjustment by the subject.

In initial tests, subjects typically spent approximately 10% of the time periodically scanning the VSD and 90% of the time conducting the visual search task. Each head-down scan lasted approximately 1-2 sec on average. Flight experts within AL/CFHI deemed this ratio of head-up/head-down time to be representative of a typical CAP scenario.

Contrail detection task. The primary task in the experiment was to perform the visual search for simulated aircraft contrails. While flying the simulator, subjects were instructed to visually search the projection screen for aircraft contrails and to respond as quickly as possible when they saw one. This task involved both a cued condition and an uncued condition, described below.

a. Uncued detection. During each trial, the subject saw only one contrail, which was presented against a solid, sky-blue background. At the onset of each trial, all three projectors projected only the background on their respective section of the screen. After an interval of 1 second, one of the optical disk players would present a faint (sub-threshold) contrail against the background. After an interval of 8 seconds, it would increase in contrast to the second level in the series. After another interval of 8 seconds, the contrail/background contrast would again

increase. This process continued until the subject responded that he/she saw a contrail or until the trial timed out.

Prior to experimentation, pilot testing was conducted to select ranges of contrast levels for presentation with each experimental condition. The maximum contrast level in each condition was defined through the pilot testing as the lowest contrast value at which the contrail was always detected. The remaining values are in six equal steps between zero and the maximum value. Table 2.1 shows the contrast values selected for presentation during the experiment. The same levels were used in both cueing conditions. The contrast increments were sufficiently small that the sudden change in contrast was not conspicuous enough to draw one's attention to it. Thus, contrast detection could be confidently attributed to spatial contrast detection rather than temporal detection mechanisms.

When detecting a contrail, subjects responded by pressing one of three buttons on a mouse. They were instructed to press the left, center, or right mouse button to indicate that the contrail was on the left, center, or right section of the screen respectively. Asking subjects to identify the location of the contrail on the screen served to ensure that the contrail had actually been detected. At the time the subject responded, the current contrast value and the accuracy of the location designation was recorded. The next trial was then initiated. If, after seven increases in contrail contrast the subject had not detected the contrail, the trial was timed out and the subsequent trial was initiated. On those trials in which the subject failed to detect the contrail, the threshold was conservatively recorded as being the highest contrast level that was presented. Trials in which the subjects responded but failed to accurately locate the contrail were repeated at the end of the session such that there was either an accurate detection or a time out associated with every trial.

Table 2.1. Contrast Values Presented for Each Experimental Condition

		Contrail/Sky Contrast		
		LENGTH		
WIDTH	LEVEL	2°	6°	10°
	1	.020	.010	.010
	2	.040	.020	.020
	3	.060	.030	.030
5 arc min.	4	.080	.040	.040
	5	.100	.050	.050
	6	.120	.060	.060
	7	.140	.070	.070
	1	.015	.010	.0075
	2	.030	.020	.0150
	3	.045	.030	.0225
15 arc min.	4	.060	.040	.0300
	5	.075	.050	.0375
	6	.090	.060	.0450
	7	.105	.070	.0525
	1	.010	.005	.005
	2	.020	.010	.010
	3	.030	.015	.015
25 arc min.	4	.040	.020	.020
	5	.050	.025	.025
	6	.060	.030	.030
	7	.070	.035	.035

b. Cued detection. The *cued* data collection task was similar to the uncued task, however, there were two variations. First, prior to the onset of each trial, the experimenter would issue a verbal cue to the subject that the contrail would appear at 10 o'clock, 12 o'clock or 2 o'clock in the visual field. This

allowed the subject to focus his search on only one of the three sections of screen, reducing the visual search area from approximately $135^{\circ} \times 37^{\circ}$ to $45^{\circ} \times 37^{\circ}$. This condition was referred to as the *cued* condition because the subject was given a general idea (within 45°) of where the contrail was located. (This should not be confused with a situation in which the subject knows *exactly* where to look for the stimulus, which is the case with more traditional threshold detection studies.) The second variation was in the subject's response. Because the approximate location of the contrail was known in advance, identification of the left, center, or right screen position was no longer a valid means of verifying actual detection of the contrail. Therefore, after responding, subjects were asked to verbally describe the position of the contrail on the screen. The experimenter, knowing the contrail position, would then make a judgment as to whether the subject actually detected the contrail.

Data Collection Procedure. After receiving instructions and contrast sensitivity screening, the subject was seated in the cockpit of the P&ES. In this position, the subject's eyes were positioned approximately 12 ft. from the center of each section of the screen, and the entire screen spanned an angular subtense of 135° .

Once in the cockpit, the subject was familiarized with the stick, throttle and rudder pedals as well as the VSD. After becoming familiar with the cockpit, the subject was allowed to fly the simulation until he/she felt comfortable with the task. Once the subject had shown competence in the flight task, he/she was asked to again fly the practice flight simulation as the contrail detection task was introduced. While maintaining the desired flight profile, the subject was asked to visually search the projection screen looking for the appearance of contrails and to respond upon detecting a contrail. A total of six practice trials were presented. At the end of the six practice trials, the subject was given the opportunity to repeat the practice trials or to proceed to the data collection trials.

Using the procedures described above, each subject performed two blocks of 60 trials. These trials consisted of the following:

Cued Block	6	Cued practice trials
	54	Cued data collection trials
Uncued Block	6	Uncued practice trials
	54	Uncued data collection trials
	120	Total Trials

The order of block presentation was counterbalanced across the twenty subjects such that ten subjects received the cued condition first and ten received the uncued condition first. Between blocks, subjects were given a five minute break to minimize fatigue and eye strain. Within each block of 54 data collection trials, six repetitions of the nine combinations of length and width were presented in random order.

SECTION III. RESULTS

Descriptive and Inferential Statistics

Measures of luminance contrast at detection for each of the eighteen conditions were averaged across repetitions and subjects. Over the course of the 2160 data collection trials, 67 trials (3.1%) resulted in time-outs, where subjects did not detect the contrail even at the highest contrast level. On these trials, contrast at detection was conservatively assigned to be that of the highest contrast level presented. Mean contrast at detection is shown in Table 3.1 for each of the eighteen experimental conditions.

Table 3.1. Mean Luminance Contrast at Detection

	Length					
Uncued	2°		6°		10°	
Width (arc min.)	mean	std dev.	mean	std dev.	mean	std dev.
5	11.58	1.053	6.05	.583	5.77	.560
15	6.99	.988	4.38	.556	3.64	.391
25	5.93	.335	3.00	.310	2.74	.267
Cued	2°		6°		10°	
Width (arc min.)	mean	std dev.	mean	std dev.	mean	std dev.
5	10.07	1.111	5.55	.682	4.93	.849
15	5.93	.896	3.69	.444	2.93	.436
25	5.44	.588	2.59	.334	2.38	.272

As expected, detection thresholds for the simulated contrails decreased as a function of width, length and cueing. Thresholds were found to be higher for uncued contrail detection than for cued detection. This difference, shown in Figure 3.1, was found to be significant using a paired-comparison T-test ($t=13.18$, $P(T \leq t) \text{ two-tail} < .0001$). Subsequent inferential analysis of the threshold data was carried out separately for the uncued and cued conditions using a two-factor

analysis of variance (ANOVA). In both cueing conditions, the ANOVA revealed significant main effects of both contrail width and length: (contrail width, uncued, $F(2,38) = 562$, $p < .0001$; contrail length, uncued, $F(2,38) = 139$, $p < .0001$; contrail width, cued, $F(2,38) = 686$, $p < .0001$; contrail length, cued, $F(2,38) = 120$, $p < .0001$). For both cueing conditions, a Tukey-pairwise comparison post-hoc test revealed that thresholds for the three levels of width differed significantly from each other, as did thresholds for the three levels of length. For both width and length, detection thresholds decreased as a function of increasing size. The main effect of width in the cued and uncued conditions is shown in Figure 3.2a and b respectively. Figure 3.2c and d illustrate the main effect of contrail length for each cueing condition. The ANOVAs also revealed significant interactions between width and length for both cueing conditions: (uncued, $F(4,76) = 79.98$, $p < .0001$; cued $F(4,76) = 54.31$, $p < .0001$), shown in Figure 3.3a and b. Examining these plots, it appears that the effect of increasing width from 5 to 15 arc minutes is greatest for the shortest contrail length (2°).

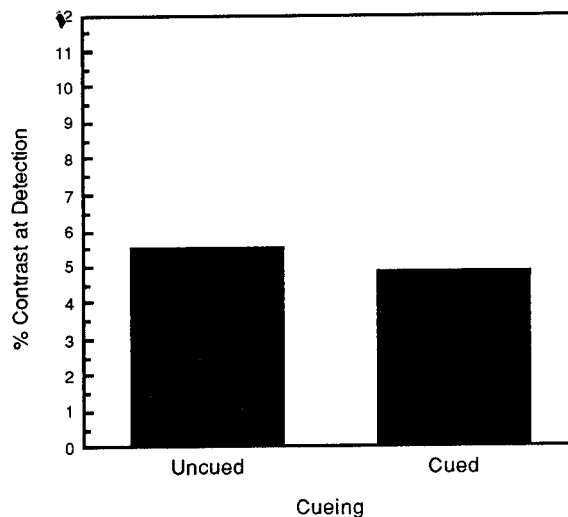


Figure 3.1. Main Effect of Cueing

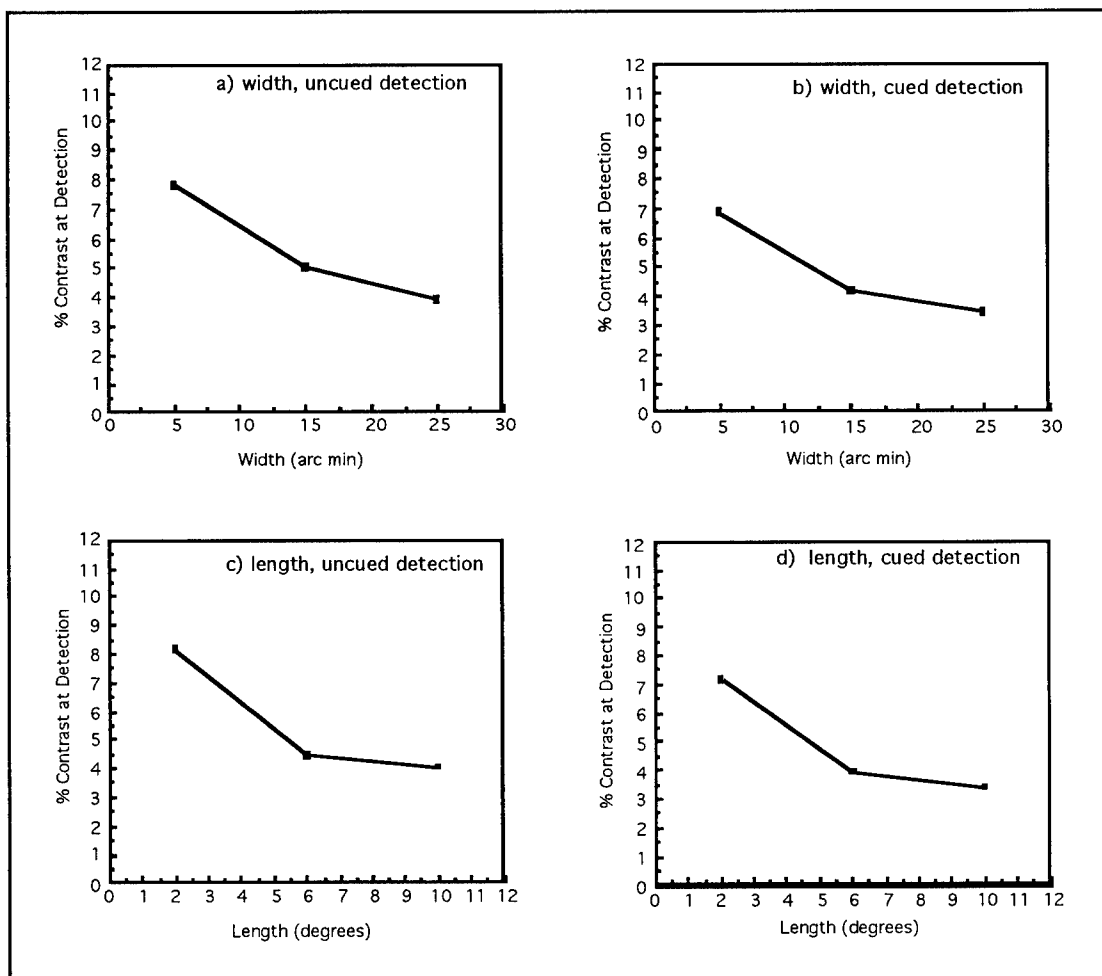


Figure 3.2. Main Effects of Width (a and b) and Length (c and d)

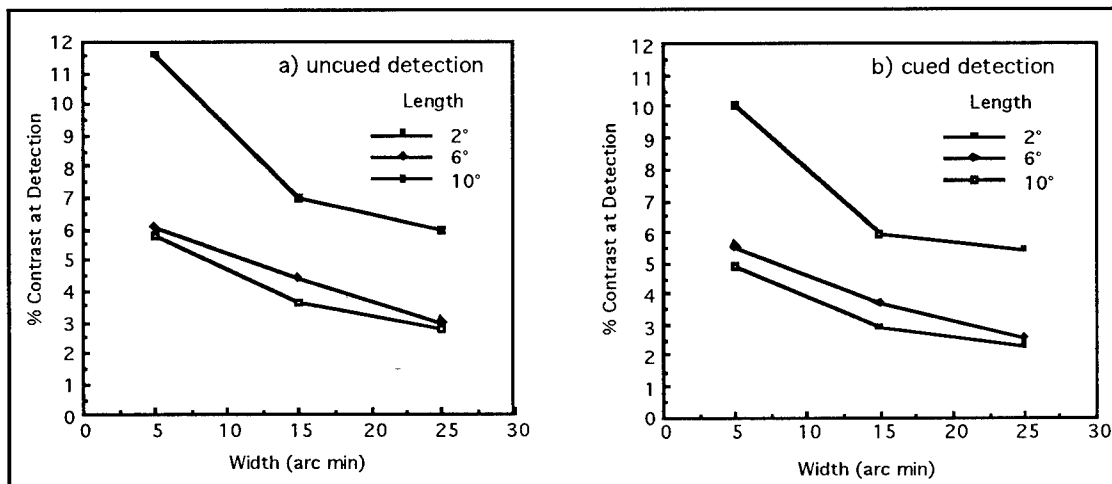


Figure 3.3. Interactions Between Contrail Width and Length for Uncued (a) and Cued (b) Detection

Psychometric Functions

Further analysis of the threshold data involved examining the probability of detection associated with a given contrast level. Often it is of interest to know the probability of detection associated with a stimulus of a given size and contrast. This type of data falls into a class of detection phenomena that was first modeled by Quick (1974), who showed that an exponential equation could be used to accurately model detection. Quick's equation is expressed as:

$$F = 1 - 2^{-(SC^\beta)} \quad \text{Eq. 3.1}$$

Where: F is the Probability of detection, C is the target to background contrast, and S and β are adjustable parameters representing sensitivity and slope respectively. In the typical detection paradigm, the Quick equation yields an "S"-shaped psychometric function describing probability of detection as a function of stimulus intensity, and it has been shown to provide good fits to empirically-obtained frequency of seeing data (Graham, Robson, & Nachmias, 1978; Legge, 1979; Nachmias, 1981; Watson & Nachmias, 1980). In addition, because the equation consistently yields the "S"-shaped curve, it is relatively easy to develop a single psychometric function across multiple observers that represents a best estimate of the population.

To develop probability of detection estimates for each of the experimental conditions, the percentage of accurate detections associated with each of the seven contrast levels was calculated. These contrast levels and the corresponding percentage of detections at each level were then input into the Quick equation representing the variables F and C respectively. Subsequently, the values of variables S and β were manipulated iteratively until they yielded an asymptotic minimum mean square error with regard to the data collected. Figures 3.4 and 3.5 show the curves predicted by the Quick equation plotted through the actual data points for the uncued and cued viewing conditions respectively. The S and β values obtained with the least squares technique are shown above each curve in Figures 3.4 and 3.5 and are also listed in Table 3.2 for each of the eighteen conditions.

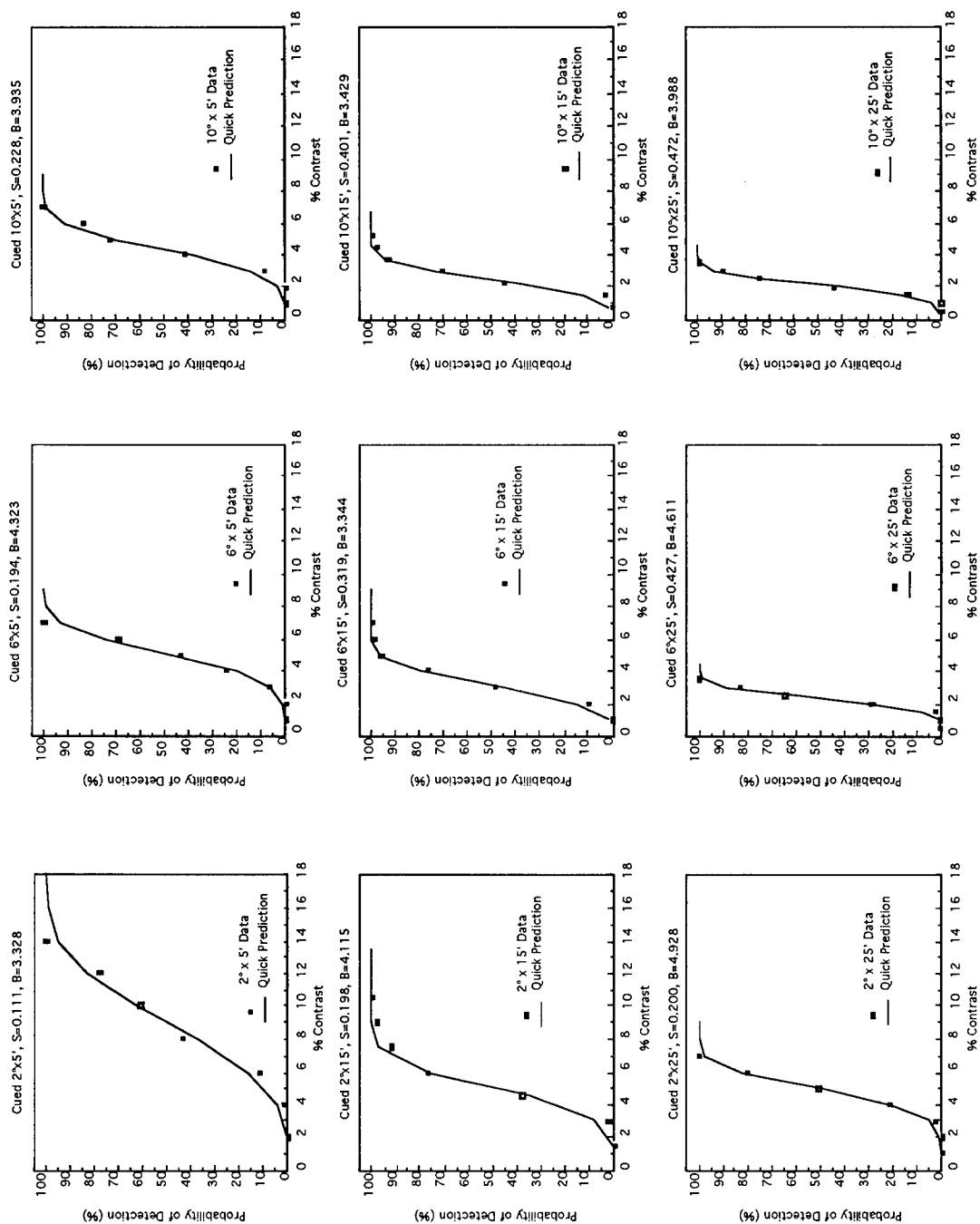


Figure 3.4. Psychometric Data and Quick Curves for Uncued Condition

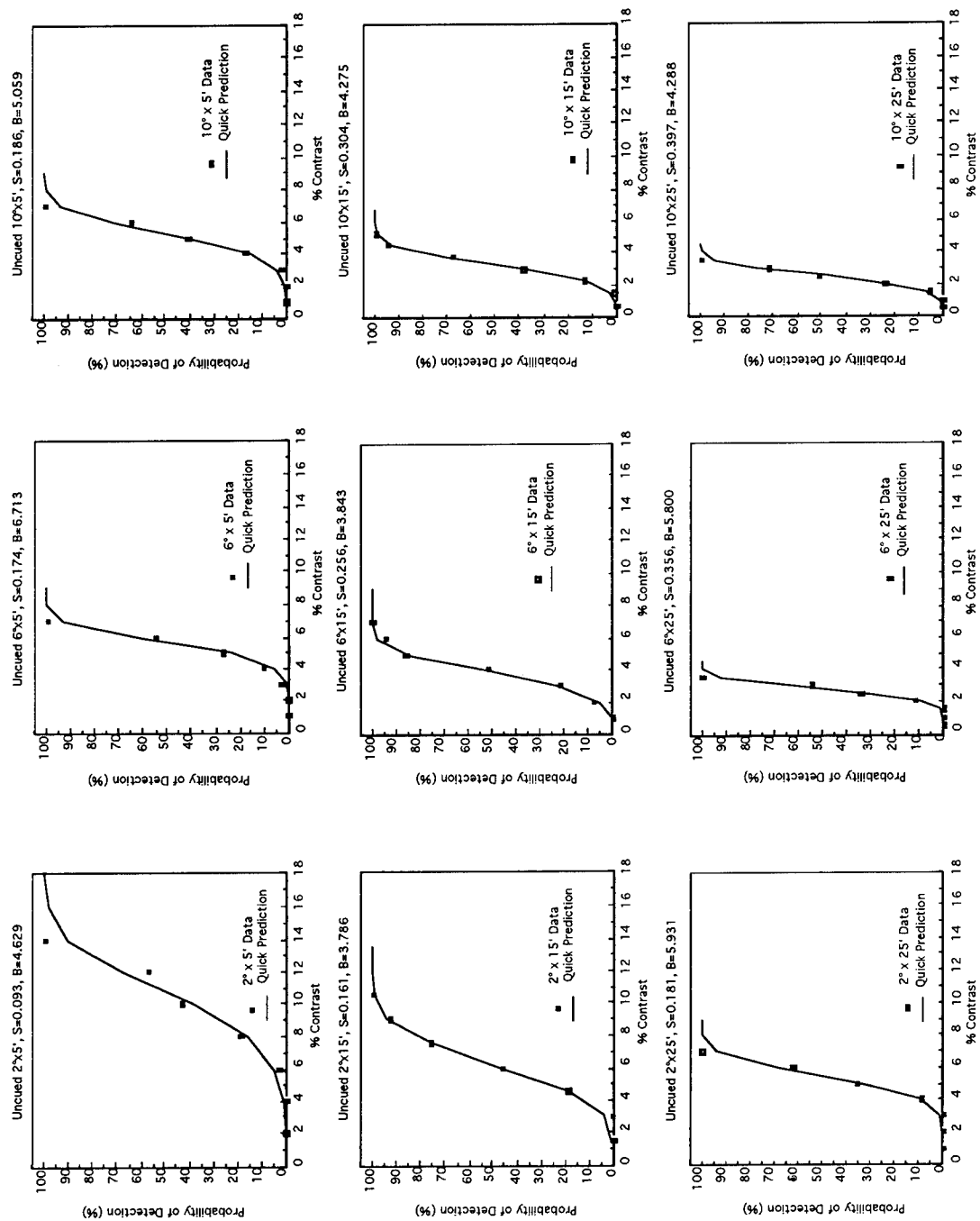


Figure 3.5. Psychometric Data and Quick Curves for Cued Condition

Table 3.2. S and β Values for Each Experimental Condition.

Length	Width	Cueing	S	β
2°	5'	No	0.093	4.629
6°	5'	No	0.174	6.713
10°	5'	No	0.186	5.059
2°	15'	No	0.161	3.786
6°	15'	No	0.256	3.843
10°	15'	No	0.304	4.075
2°	25'	No	0.181	5.931
6°	25'	No	0.356	5.800
10°	25'	No	0.397	4.288
2°	5'	Yes	0.111	3.328
6°	5'	Yes	0.194	4.322
10°	5'	Yes	0.228	3.935
2°	15'	Yes	0.198	4.115
6°	15'	Yes	0.319	3.343
10°	15'	Yes	0.401	3.423
2°	25'	Yes	0.200	4.279
6°	25'	Yes	0.427	4.611
10°	25'	Yes	0.471	3.988

SECTION IV. DISCUSSION

The primary goal of the current study was to quantify visual detection of aircraft contrails within a given scenario. The results described above generally demonstrate characteristics of visual detection that have been observed in previous research. However, certain deviations from previous findings were observed. These similarities and differences are described below and their implications discussed.

To simplify comparison with previous research, the current stimulus conditions can be expressed in terms of stimulus area rather than stimulus width and length. Figures 4.1a and 4.1b plot thresholds for detection as a function of contrail area in terms of square minutes of arc for the uncued and cued conditions respectively. Each line in these plots shows the progression across increasing lengths for a given width condition.

Threshold Values

Thresholds for contrast at detection were found to be somewhat higher than those found in previous detection studies. Blackwell (1946) found thresholds for circular targets 121 arc minutes in diameter (11500 square arc min. in area) to be approximately 0.8%. However, examining Figure 4.1b, we find that the current study yielded thresholds for stimuli of this size of approximately 2.5%. Similarly, although Lamar et. al. (1947) found contrast thresholds of 1.41% for rectangular targets 800 square arc minutes in area, thresholds for a corresponding target size in the current study approached 9%.

Effect of Stimulus Area

Another aspect in which results of the current study differ from those of previous research is the degree to which thresholds are impacted by stimulus size. It has been well documented that contrast thresholds decrease as stimulus area increases and that this relationship diminishes reaching an asymptotic value as stimulus area continues to increase (Boff & Lincoln, 1988).

The current results support this notion for stimuli in the contrail domain. As contrails increase in size, they can be detected at lower and lower contrast levels. This is true for increases in both width and length across the levels tested. Referring back to Figure 3.3, it can be seen that the effect of increasing stimulus size diminishes for the larger stimuli presented. That is, thresholds were shown to decrease much more when length was increased from 2° to 6° than they did when length was increased from 6° to 10° . Similarly, increasing width from 5 to 15 arc min. produced greater decreases in threshold than increasing width from 15 to 25 arc min. The interaction between width and length seems to suggest that the largest effect of increasing width is associated with the shortest and narrowest (i.e. smallest) contrails. Although there are diminished reductions in threshold associated with these increases in width and length, the reductions do not appear to approach asymptote until reaching the largest stimuli used in this study. This finding is somewhat inconsistent with findings from Lamar et. al. (1947) discussed earlier. Examining threshold as a function of stimulus area in Figure 4.1, it can be seen that detection thresholds do not reach asymptote until stimulus area exceeds approximately 8500 square arc minutes. In the Lamar et. al. (1947) study, however, detection thresholds became asymptotic for rectangular stimuli with areas as small as 100 square arc minutes.

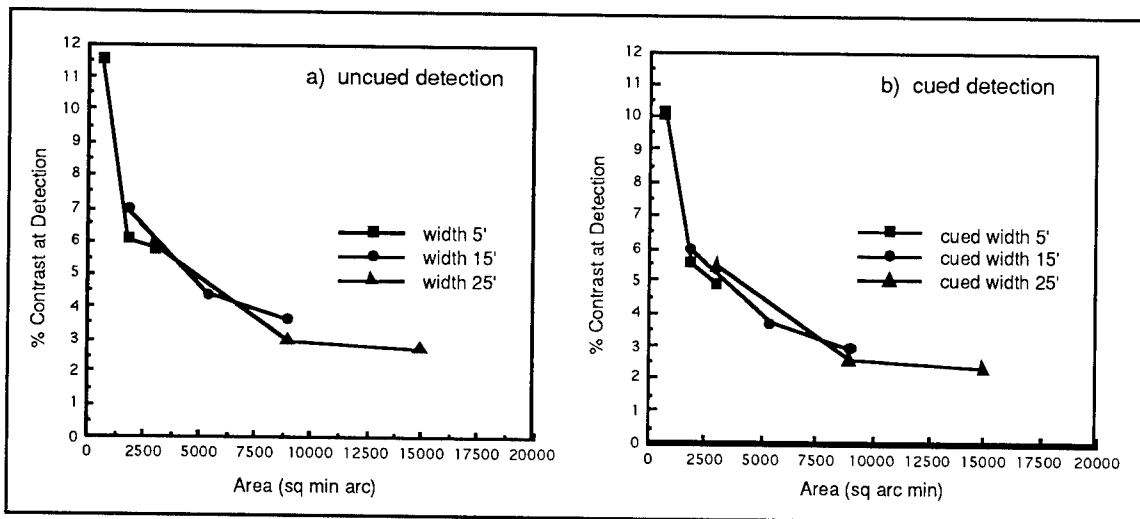


Figure 4.1. Detection Threshold as a Function of Contrail Area for Uncued (a) and Cued (b) Detection

It is not surprising that the current detection thresholds were found to be higher and to exhibit slightly different threshold x area relationships than those in previous research. Typically, research on visual detection has been conducted in a setting designed to maximize detection. Perhaps the most salient difference between the current experimental approach and that of contrast detection studies in the past is the use of precise location cueing in previous studies. Observers are typically instructed to focus on an orientation or fixation point just prior to the stimulus onset. This cue is intended to draw the subject's focus to the immediate location of the target to be detected, thereby eliminating the need for conducting a visual search and isolating the contrast detection mechanisms of the visual system. Both the Blackwell (1946) and Lamar et. al. (1947) studies used orientation points to cue the observer's to the stimuli position within 3° and 2° respectively. As discussed earlier in this paper, however, the detection of contrails in an air-to-air environment is not a task that can be accurately modeled using a precise cueing approach. That is, in the given scenario, in which a pilot is attempting to visually locate and intercept another contrail-producing aircraft, the pilot will not know the precise location in which to look in anticipation of detecting the aircraft contrail. At best, the pilot would know the *general direction* in which he would expect to see the contrail (what we are calling "cued" detection), and in many cases, he would be searching his entire field of view ("uncued" detection). It is likely that the differences observed between thresholds in the current and previous research can be attributed to the fact that subjects were never oriented to the exact location of the target (within 2° or 3°), but rather had to perform a visual search across an area measuring $45^\circ \times 37^\circ$ in the cued condition and $135^\circ \times 37^\circ$ in the uncued condition.

In addition, subjects in the current study were not able to devote 100% of their time to the visual detection task. In order to simulate a realistic scenario, they were forced to periodically interrupt the visual search to look down and scan the instruments. Although it was observed that subjects generally spent only 10% of the time scanning the instruments and 90% conducting the visual search task, the intermittent interruptions may have served to increase the detection thresholds.

Finally, another factor that may be responsible for a portion of the difference between thresholds observed in the current study and those obtained in previous research is the degree of observer training. Subjects in the current study each participated in a single experimental session, performing a total of 12 practice trials and 108 data collection trials. Though perceptual tasks such as this are quite simple to perform, observers can perform at higher levels with a good deal of training. For example, observers in the Blackwell (1946) study were full-time employees who had worked between six months and two and one half years participating in detection studies, with approximately half of their time being spent observing stimuli. It was estimated that prior to the actual data collection, subjects had performed between 35,000 and 75,000 observations each. This degree of training, while leading to lower detection thresholds for a given task, was not considered necessary nor appropriate for observers considering the detection scenario being modeled.

Generalizability

The factors described above were deliberately introduced into the experimental design in order to achieve a realistic scenario and to increase the generalizability of the results. However, one aspect of real-world viewing that it failed to model is full daylight adaptation. The contrail detection task was conducted using only room lighting levels. Theoretically, this may impact the generalizability of the results to the daylight search scenario that was intended to be modeled. However, previous research indicates that the effect of adaptive luminance level may be minimal across the range of room lighting to full daylight. Blackwell (1946) found that contrast at detection decreased with increasing light levels until it became constant at around 1.0 footlambert. However, he found *no* change in detection threshold with adaptive luminance levels greater than 1.0 footlambert. The adaptive luminance level in the current study was 2.11 footlamberts, indicating that although there is over a three order-of-magnitude difference between the current lighting level and true daylight conditions, the threshold data obtained may be safely generalized to daylight conditions.

It should be restated that the current study provides a conservative estimate of contrail contrast at detection. This is a result of using a uniform blue background. Often the sky will not be a uniform blue color, but rather it will be spotted with

gray or white clouds that will serve as distracters or decrease contrast. In addition, subjects in the current study viewed the contrails directly. In an operational setting, apparent contrail contrast may be further attenuated by the aircraft canopy and by aircrew visors.

Based upon the high fidelity and conservative nature of the experimental scenario, researchers feel confident that the results presented here provide a reasonable worst-case estimate of the contrast thresholds associated with the detection of aircraft contrails. Therefore, until contrail detection data can be collected in an operational environment, the current data and results are thought to be adequate for generalization to real-world contrail detection. The final section of this document provides additional information that will aid in extrapolation of this data to predict thresholds across a range of possible conditions.

SECTION V. EXTRAPOLATION AND PREDICTION

This section is intended to allow the reader to interpolate across the current data and to predict the probability of detection associated with given contrail characteristics. As stated earlier, the current effort investigated only the luminance contrast aspect of contrail detection. Thus, additional pieces of information are necessary to fully characterize contrail detection. These include the size of the contrail being emitted, the distance between the contrail and the observer, and the estimated contrail/sky luminance contrast at that distance. Given this information, estimates of contrail detectability can be made using the following information.

The results from the current study indicate that the length to width ratio of a contrail did not impact the contrast required for detection. Thus, contrail size can be viewed simply as the area subtended by the contrail rather than by its individual width and length dimensions. This study investigated contrail sizes ranging from 600 sq min of arc to 15000 sq min. The reader, however, may be interested in extrapolating contrast thresholds for smaller contrail areas such as those associated with a contrail 1 arc min in width. Such extrapolation was accomplished by fitting the area to a square root equation known as Piper's Law.

Although the current data seem to suggest that contrast detection thresholds continue to decrease with increasing field sizes beyond those determined by Lamar et. al (1947), they appear to be described well by Piper's law (Eq. 1.2). The mean area data was fit with Piper's law by the same iterative least squares technique used to fit the Quick equation to the psychometric data. The resulting curves and the constant values used to create those curves are shown in Figure 5.1 and Table 5.1 respectively. These plots, showing logarithmic increases on the X and Y axes, enable easier extrapolation of the data down to smaller contrails than were used in the current investigation. The best fit of the Piper equation to the current data yielded a constant (k) value of 2.92 for the uncued viewing condition and 2.54 for cued viewing. Although the current investigation addressed contrails down to 5 arc min in width, viewing conditions may occur that produce contrails as narrow as 1.0 arc min. Using a fit of Piper's law to the current data, thresholds for contrails 1.0 arc min wide are predicted for the 2°, 6°

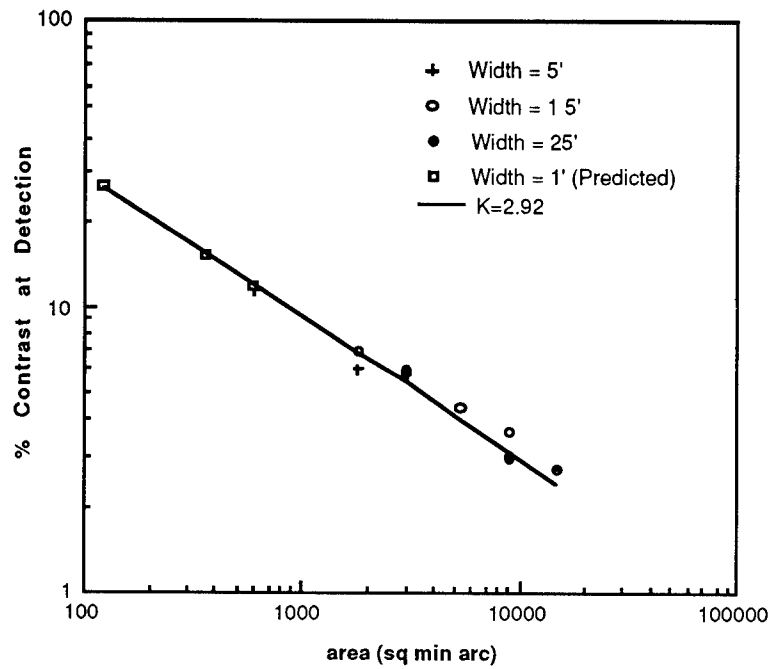
and 10° length conditions used in the current study, corresponding to contrail areas of 120, 360, and 600 square minutes of arc. This extrapolation is also shown in Figure 5.1 and Table 5.1.

Again, it may be of interest to use the current data to estimate contrail contrast values associated with a range of probabilities of detection. While the above data gives the contrast at mean detection, it is not helpful when predicting the contrast required for other probabilities of detection. This issue can be addressed, however, by analyzing threshold estimates from the Quick predictions associated with the mean data. For example, to estimate the contrast level associated with a 10% probability of detection for a given stimulus size, the Piper equation can be fit to the threshold estimates yielded by the Quick equation for each of the conditions tested. The resulting curves, plotted with logarithmic increases on the X and Y axes, indicate a predicted contrast required for 10% detection across a range of stimulus sizes. The prediction curves for a 10% probability of detection are plotted in Figure 5.2. This approach was repeated to determine curves associated with 50% and 100% detection. The resulting curves are depicted in Figures 5.3 and 5.4 respectively.

Table 5.1. K Constants for Detection Criteria.

Detection Criteria	Cueing	K
Mean	Uncued	2.94
Mean	Cued	2.54
100%	Uncued	4.45
100%	Cued	4.27
50%	Uncued	2.71
50%	Cued	2.27
10%	Uncued	1.83
10%	Cued	1.38

Uncued Mean Detection



Cued Mean Detection

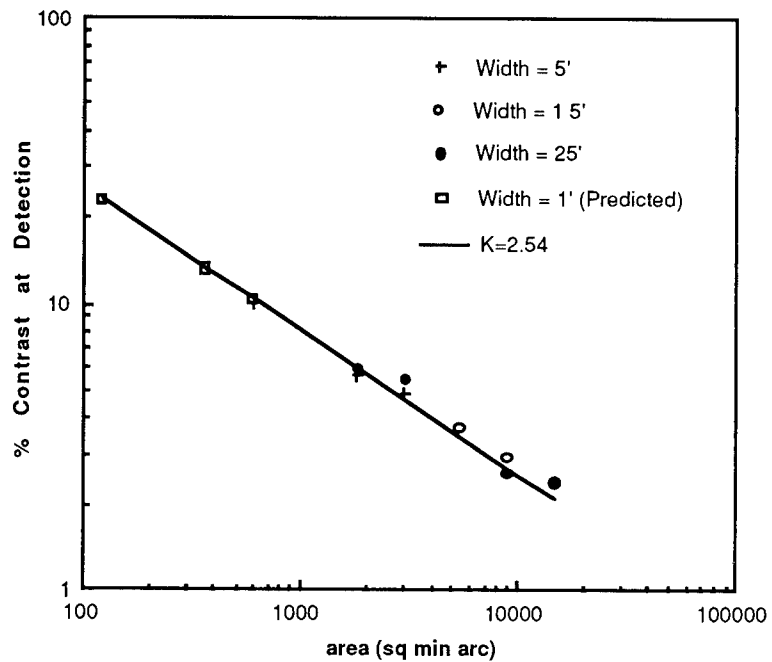
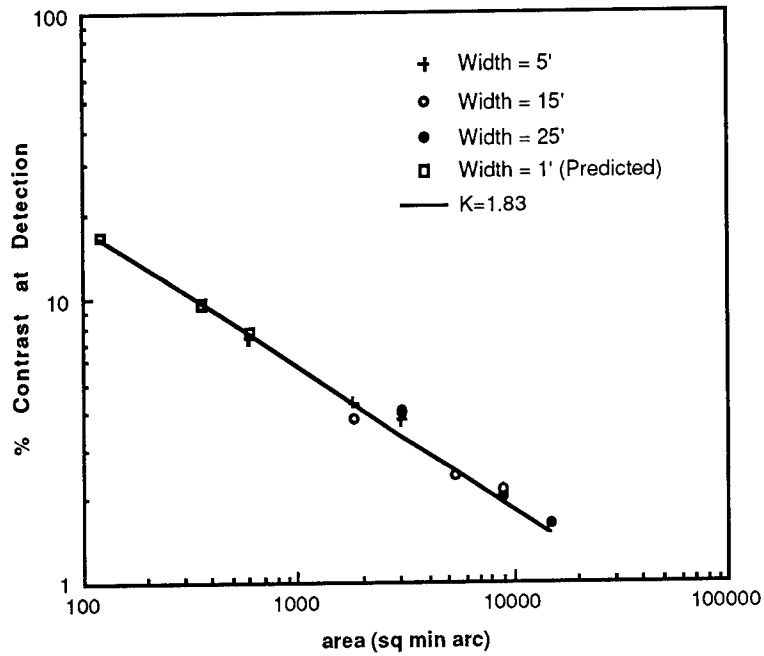


Figure 5.1. Mean Thresholds at Detection for the Experimental Conditions and Extrapolated to 1 Arc Min Using a Best Fit to Piper's Equation

Uncued 10% Detection



Cued 10% Detection

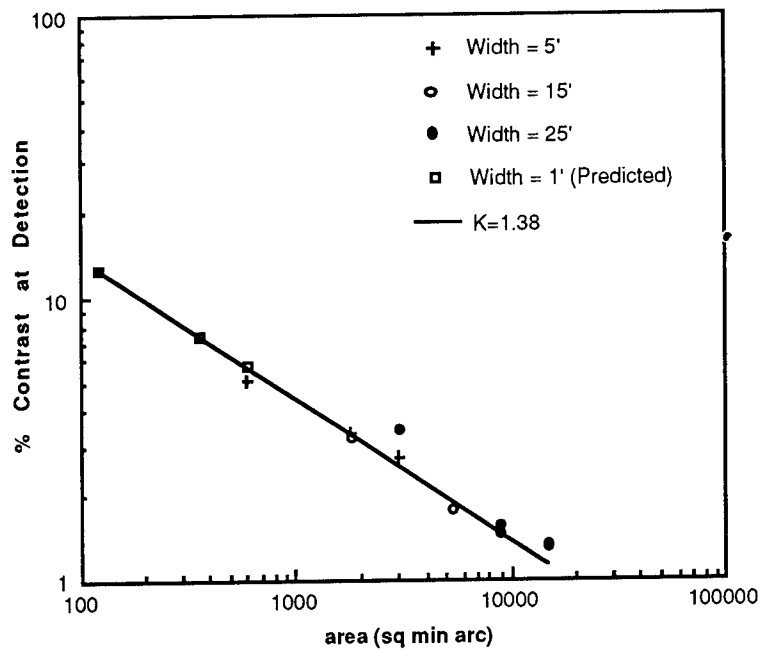
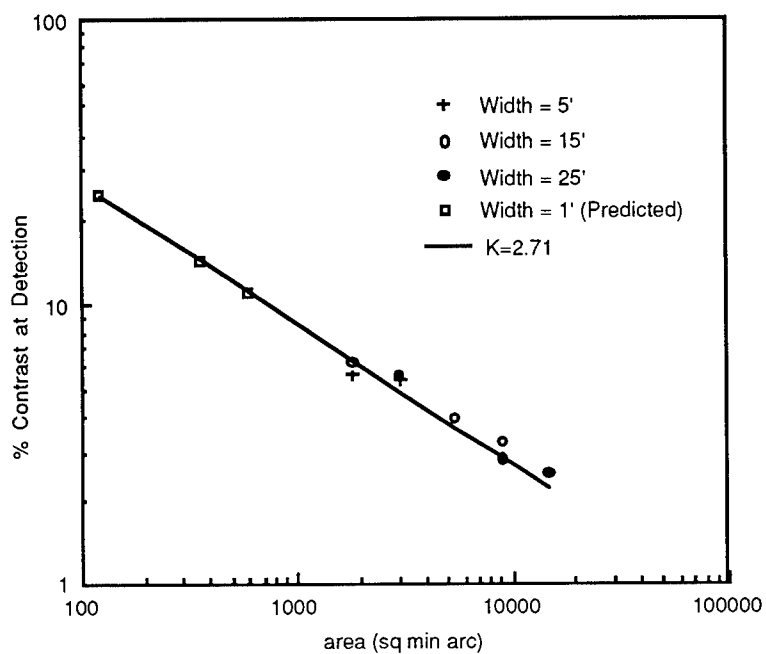


Figure 5.2. Predicted 10% Probability of Detection Curves

Uncued 50% Detection



Cued 50% Detection

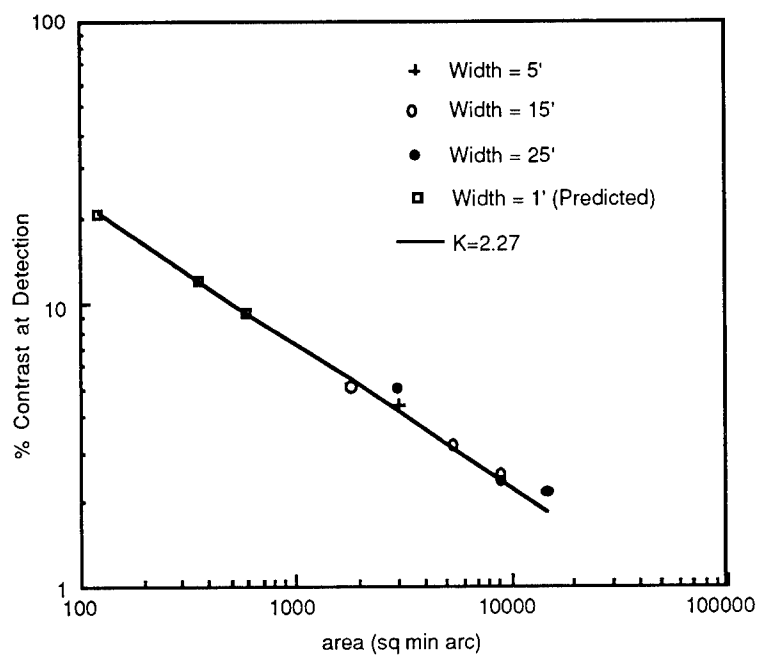


Figure 5.3. Predicted 50% Probability of Detection Curves

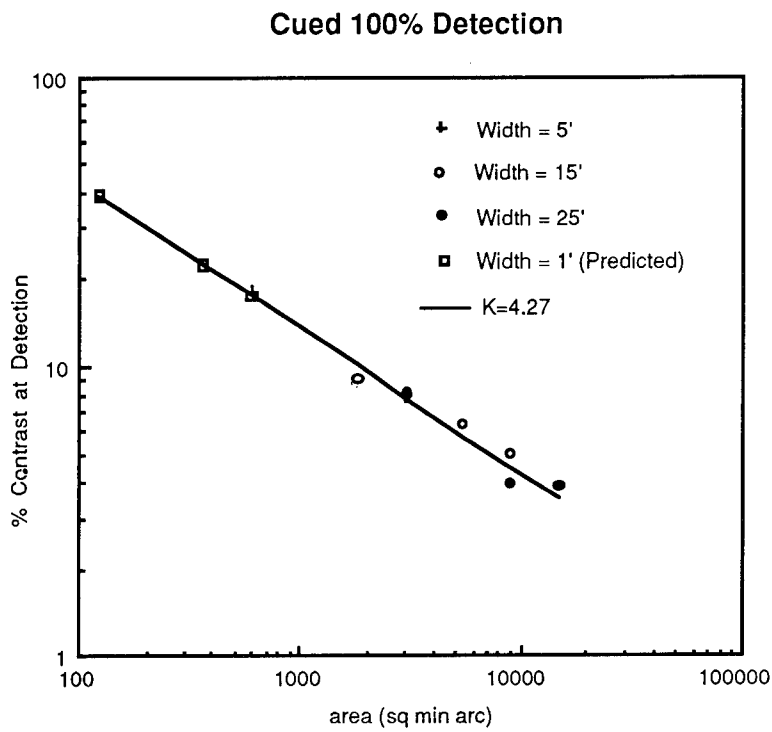
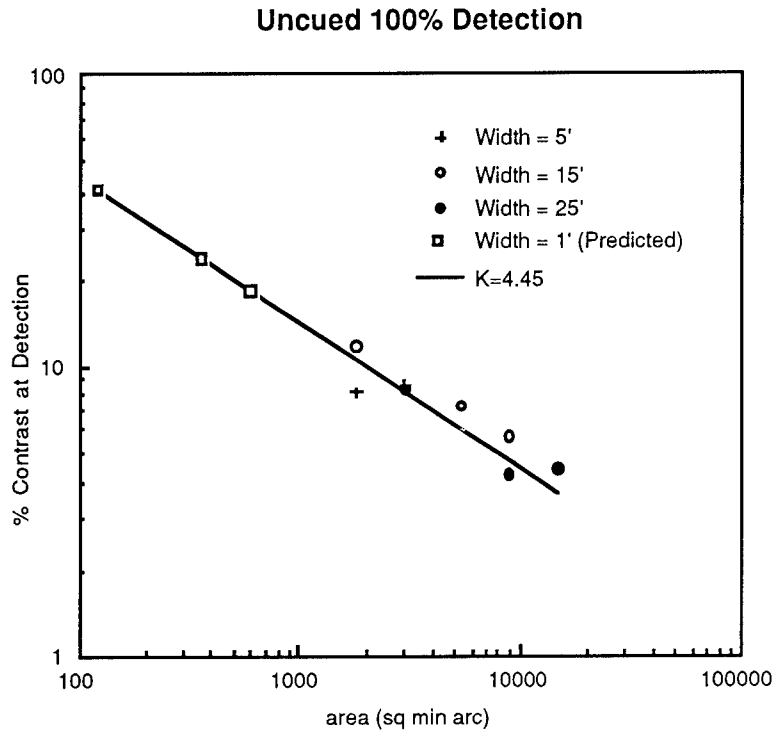


Figure 5.4. Predicted 100% Probability of Detection Curves

Although results for contrails with widths as small as one minute of arc can be extrapolated from the current data using Piper's law, there is no empirical evidence to support this extrapolation. It is proposed that one minute of arc is the thinnest contrail for which thresholds can accurately be extrapolated using this method. Contrails thinner than one minute of arc may be better fit by Ricco's law (Eq. 1.1). The experimenters caution that there is no empirical evidence indicating at which point detection transitions from performance characterized by Piper's law to that characterized by Ricco for a complex detection scenario such as that used in this study.

REFERENCES

Air Weather Service, (1981). Forecasting Aircraft Condensation Trails. (Report No. AWS/TR-81/001). Scott AFB, I.L.: Air Weather Service.

Appleman, (1953), cited in Bjornsen, (1992).

Bjornsen, B.M., (1992). SAC Contrail Formation Study. (Report No. USAFETAC/PR-92/003). Scott, AFB, I.L.; USAF Environmental Technical Applications Center.

Blackwell, H. R. (1946). Contrast thresholds of the human eye. Journal of the Optical Society of America, 36(11), 624-643.

Boff, K. R., & Lincoln, J. E., (1988). Engineering Data Compendium, Human Perception and Performance, Vol I, 246, Harry G. Armstrong Aerospace Medical Research Laboratory, Wright-Patterson AFB, OH.

Brown, E.L., and Deffenbacher, K., (1988). Perception and the Senses. New York: Oxford University Press.

Duntley, S. Q., (1948). The reduction of apparent contrast by the Atmosphere. Journal of the Optical Society of America, 38(2), 179-191.

Graham, Brown & Mote, (1939), cited in Brown & Deffenbacher, (1979).

Graham N., Robson J. G. and Nachmias, (1978). Grating summation in fovea and periphery. Vision Research. 18, 815-825.

Lamar, E. S., Hecht, S., Schlaer, S., & Hendley, C. D. (1947). Journal of the Optical Society of America, 37(7), 531-545.

Legge G. E., (1979). Spatial Frequency Masking in Human Vision: Binocular Interactions. Journal of the Optical Society of America. 69, 838-847.

Meyer-Arendt, J. R., (1972). Introduction to Classical and Modern Optics. Englewood Cliffs, N.J.: Prentice-Hall, Inc.

Nachmias J., (1981). On the Psychometric Function for Contrast Detection. Vision Research, 21, 215-223.

Overington, I., (1976). Vision and Acquisition, New York: Crane, Russak & Co..

Piper, (1903), cited in Boff & Lincoln, (1988).

Quick R. F. Jr., (1974). A Vector-Magnitude Model of Contrast Detection. Kybernetik, 16, 65-67.

RCA (1974). RCA Electro-Optics Handbook, Lancaster, P.A.: RCA.

Ricco, (1877), cited in Boff & Lincoln, (1988).

Watson A. B. and Nachmias J., (1980). Summation of Asynchronous Gratings. Vision Research, 20, 91-94.

Watson A. B., (1982). Summation of Grating Patches Indicates Many Types of Detectors at One Retinal Location. Vision Research, 22, 17-25.

Wyszecki G. and Stiles W. S., (1967). Color Science, New York: Wiley.